Received: 11 March 2021 | Revised: 4 May 2021 | Accepted: 5 May 2021

DOI: 10.1002/psp4.12660

ARTICLE

Population pharmacokinetics of belantamab mafodotin, a BCMA-targeting agent in patients with relapsed/refractory multiple myeloma

Chetan Rathi[1] | **Jon Collins**[2] | **Herbert Struemper**[2] | **Joanna Opalinska**[1] | **Roxanne C. Jewell**[2] | **Geraldine Ferron-Brady**[1]

[1]GlaxoSmithKline, Collegeville, Pennsylvania, USA

[2]GlaxoSmithKline, Research Triangle Park, North Carolina, USA

Correspondence
Geraldine Ferron-Brady, GlaxoSmithKline, 1000 Black Rock Road, Collegeville, PA 19426, USA.
Email: geraldine.x.ferron@gsk.com

Funding information
These studies and analyses were funded by GlaxoSmithKline (GSK Study numbers: 117159 and 205678).

Abstract

Belantamab mafodotin (belamaf) is an antibody–drug conjugate (ADC) targeting B-cell maturation antigen (BCMA). Nonlinear mixed-effects models were developed to characterize the population pharmacokinetics (PopPK) of ADC, total monoclonal antibody (mAb), and cysteine-maleimidocaproyl-MMAF (cys-mcMMAF) after 0.03–4.6 mg/kg dosing every 3 weeks in heavily pretreated patients with relapsed/refractory multiple myeloma (RRMM; DREAMM-1, $n = 73$; DREAMM-2, $n = 218$). Sequential modeling methodology was used. Individual *post hoc* parameter estimates from the final ADC model were used to develop total mAb and cys-mcMMAF models. Formal covariate selection used a modified stepwise forward inclusion method with backward elimination. A linear, two-compartment PopPK model with a time-varying clearance (CL) described ADC PK. Initial ADC typical value for CL for a DREAMM-2 patient was 0.936 L/day with a half-life of 11.5 days, over time CL was reduced by 28% resulting in a half-life of 14.3 days. Time to 50% maximal CL change was ~ 50 days. Baseline soluble BCMA (sBCMA), immunoglobulin (IgG), albumin, and bodyweight impacted ADC CL. Cys-mcMMAF concentrations were described with a linear two-compartment model linked to ADC; input rate was governed by deconjugation/intracellular proteolytic degradation of ADC represented by an exponentially decreasing MMAF:mAb (drug antibody ratio [DAR]) after each dose. Time to 50% DAR reduction was 10.3 days. Baseline sBCMA and IgG impacted cys-mcMMAF central volume of distribution. In conclusion, ADC, total mAb, and cys-mcMMAF concentration–time profiles in RRMM were well-described by PopPK models, and exposure was most strongly impacted by disease-related characteristics.

Study Highlights

WHAT IS THE CURRENT KNOWLEDGE ON THE TOPIC?

This is the first published population pharmacokinetic (PopPK) modeling analysis of belantamab mafodotin (belamaf), a monomethyl auristatin F (MMAF)-containing

Chetan Rathi and Jon Collins are joint first authors.

antibody–drug conjugate (ADC) recently approved to treat relapsed/refractory multiple myeloma (RRMM).

WHAT QUESTION DID THIS STUDY ADDRESS?

PopPK models utilizing phase I and pivotal phase II study data in heavily pretreated patients with RRMM were developed to evaluate exposure parameters for belamaf, total monoclonal antibody (total mAb), and cysteine-maleimidocaproyl-MMAF (cys-mcMMAF). Significant clinical covariates impacting PK parameters and exposure were identified.

WHAT DOES THIS STUDY ADD TO OUR KNOWLEDGE?

PK of belamaf, total mAb, and cys-mcMMAF were well-characterized in patients with RRMM by linear, two-compartment models with time-varying clearance for ADC and time-varying drug antibody ratio for cys-mcMMAF. Disease-related characteristics were most associated with exposure.

HOW MIGHT THIS CHANGE DRUG DISCOVERY, DEVELOPMENT, AND OR THERAPEUTICS?

These models improve our understanding of belamaf ADC, total mAb, and cys-mcMMAF PK and the clinical impact of key covariates. This knowledge will support ongoing clinical development and inform dosing strategies for future belamaf studies.

INTRODUCTION

Belantamab mafodotin (belamaf; BLENREP; GlaxoSmithKline, Brentford, UK) is first-in-class antibody–drug conjugate (ADC) recently approved in the United States and Europe for the treatment of relapsed/refractory multiple myeloma (RRMM) after greater than or equal to 4 prior therapies.[1,2] It targets B-cell maturation antigen (BCMA), a cell membrane receptor expressed on all malignant plasma cells, which is essential for their proliferation and survival.[3,4] Belamaf comprises an afucosylated humanized immunoglobulin G1 (IgG1) anti-BCMA monoclonal antibody (mAb) conjugated to a microtubule-disrupting agent, monomethyl auristatin-F (MMAF), by a protease-resistant maleimidocaproyl (mc) linker. Belamaf binds to BCMA, eliminating multiple myeloma (MM) cells by a multimodal mechanism.[4] Delivery of MMAF to MM cells leads to: (1) immune-independent ADC-mediated apoptosis and release of markers characteristic of immunogenic cell death, and (2) immune-dependent antibody-dependent cellular cytotoxicity/phagocytosis.[4,5]

In both the phase I DREAMM-1 (NCT02064387) and pivotal, phase II DREAMM-2 (NCT03525678) studies, single-agent belamaf induced deep and durable clinical responses with an acceptable safety profile in patients with heavily pretreated RRMM.[6–8]

The aim of this analysis was to characterize the clinical pharmacokinetics (PK) of single-agent belamaf in patients with heavily pretreated RRMM. We describe the development of population pharmacokinetic (PopPK) models for belamaf, the total mAb, and cysteine maleimidocaproyl-MMAF (cys-mcMMAF) in patients with RRMM, and the identification of covariates of clinical relevance to exposure. Investigations of the relationships between exposure of belamaf or cys-mcMMAF with efficacy and safety end points and the identified covariates of clinical relevance are reported separately (Ferron-Brady et al., 2021; in preparation [unpublished data]).

METHODS

Study population and PK sampling

The DREAMM-1 and DREAMM-2 clinical studies provided data for the PopPK models; details of the studies have been reported previously[6–8] (summarized in Table S1). In brief, DREAMM-1 was a two-part, open-label, phase I study of belamaf (0.03–4.6 mg/kg; frozen liquid presentation) in patients with RRMM,[7] and DREAMM-2 is an ongoing open-label, two-arm, randomized phase II study of single-agent belamaf (2.5 or 3.4 mg/kg frozen liquid presentation) in heavily pretreated patients with RRMM; an independent cohort in DREAMM-2 received a lyophilized presentation of belamaf 3.4 mg/kg (same assessments and procedures as the main study). Both studies were conducted in accordance with the Declaration of Helsinki; protocols and informed consent forms were reviewed and approved by Institutional Review Boards/Independent Ethics Committees according to local guidelines.

PK data were collected from all patients with RRMM who received belamaf in DREAMM-1 ($n = 73$) and DREAMM-2 ($n = 218$; frozen liquid presentation $n = 95$ [2.5 mg/kg], $n = 99$ [3.4 mg/kg] and lyophilized presentation $n = 24$ [3.4 mg/kg]). For PK measurements, blood samples were

taken pre- and post-belamaf dose and analyzed for belamaf (ADC; free or complexed with soluble BCMA [sBCMA]), total mAb (mAb with or without cys-mcMMAF, free or complexed with sBCMA) and cys-mcMMAF concentrations (Table S1).

In DREAMM-1, ADC concentration was determined by enzyme-linked immunosorbent assay (ELISA) using (1) biotinylated anti-mcMMAF capture antibody and a mouse anti-human IgG (Fc-specific) detection antibody conjugated to horseradish peroxidase (HRP) (Part 1) and (2) an anti-mcMMAF capture antibody and a biotinylated anti-idiotypic minibody detection reagent specific for the antibody backbone portion of the ADC with streptavidin conjugated to HRP (Part 2). Total mAb concentration was determined by ELISA using an idiotypic anti-belamaf capture minibody and detected using a mouse anti-human IgG (Fc-specific) antibody conjugated to HRP. Cys-mcMMAF was assessed using the VALA method, which involved analysis by ultra-high performance liquid chromatography tandem mass spectrometry (UHPLC-MS/MS) assay.

In DREAMM-2, ADC and total mAb concentrations were determined using the same methods as in DREAMM-1 (Part 2 for ADC concentration). Cys-mcMMAF concentration was determined using an updated method (PKC) consisting of a new extraction process and a different mass transition during the UHPLC-MS/MS assay to improve selectivity and robustness. As different assays were used to determine cys-mcMMAF concentrations for DREAMM-1 and DREAMM-2, the following equation, derived from DREAMM-2 samples with quantifiable concentrations when analyzed with both methods ($n = 1301$), was implemented for the concentrations from DREAMM-1 to correct the model predictions so they could be compared with observed data:

$$\text{Conc}_{\text{DREAMM-1, VALA, ipred}} = 1.486 * \text{Conc}_{\text{DREAMM-1, PKC, ipred}} - 8.360$$

Population PK model development

Data from DREAMM-1 (cutoff August 31, 2018) and DREAMM-2 (cutoff June 21, 2019; primary analysis) were used for PopPK model development. PopPK models were developed with a nonlinear mixed-effect modeling approach using NONMEM version 7.3 (ICON Development Solutions, Ellicott City, MD, USA). Model parameters were estimated with a first order conditional estimation method for log transformed concentrations (ADC and total mAb) and with interaction for untransformed concentrations (cys-mcMMAF). The sum of ADC and naked mAb, formed via deconjugation of cys-mcMMAF using a first-order rate constant, accounted for total mAb concentration. A sequential modeling methodology was used and model development was initiated by characterizing the PK of ADC. After establishing the ADC base model, the covariate model was built and a final PopPK model was generated for ADC. Total mAb and cys-mcMMAF were modeled using individual *post hoc* ADC PK parameter estimates to predict ADC concentrations as model inputs. For ADC, a two-compartment PK model with first-order elimination parameterized in terms of clearance (CL), central volume (V1), intercompartmental CL (Q), and peripheral volume (V2) was fitted to its concentration data. Model development included the investigation of random effects, time-varying parameters, and subsequent inclusion of plausible covariates on relevant parameters.

Parameters were modeled using either log normal or normal distribution:

$$\text{Lognormal: } P_i = TVP_o * EXP\left(\eta_i\right)$$

$$\text{Normal: } P_i = TVP_o + \eta_i$$

where TVP_0 is the typical value for parameter and η_i is individual variability from the standard normal distribution N(0, ω^2).

Covariate selection was based on physiological plausibility, supported by graphical evaluation; potential covariates included demographics (eg, sex, race, age, and weight), organ function indicators (eg, albumin, alanine aminotransferase [ALT], aspartate aminotransferase [AST], bilirubin, estimated glomerular filtration rate using the Modified Diet in Renal Disease [MDRD] formula), disease-related (eg, International Staging System stage, Eastern Cooperative Oncology Group [ECOG] performance status, baseline sBCMA, and IgG), and other factors (lyophile presentation, immunogenicity, prior daratumumab treatment, and number of lines of prior therapy). Hepatic impairment was also defined using National Cancer Institute criteria.[9] Missing covariate values were imputed using study-specific median values or most frequent category. Continuous covariates were evaluated using a power function; categorical covariates were evaluated as fractional change from the typical value.

Formal covariate selection was performed using a stepwise-restricted forward addition procedure, a modified version of a conventional stepwise forward inclusion method with a backward elimination step. Covariates were added sequentially to the base model starting with those causing the largest drop in objective function value (dOFV) until subsequent covariates no longer led to dOFV of greater than or equal to 6.64 points ($p < 0.01$). Each covariate's significance was tested individually with backward elimination (dOFV <10.83; $p < 0.001$) to create the final model; a decision at one step could impact the decision made at the next step. Model codes are available in Supplementary Methods.

PopPK model evaluation

The predictive performance of the final models was assessed using visual predictive checks (VPCs) with a minimum of 500 study replicates. Binning was performed on protocol-scheduled times, as appropriate. The 95% confidence intervals (CIs) of model parameters were determined either by outputs from a successful covariance step after estimation or via re-estimation using nonparametric bootstrap with replacement with 1000 or 2000 bootstrap replicates. Bootstrap statistics were based only on replicates that minimized successfully.

Simulation of *post hoc* exposure measures

The final models for both ADC and cys-mcMMAF were used to generate *post hoc* exposure measures for all individuals in the PopPK analysis. Individual concentrations for ADC and cys-mcMMAF were simulated for cycle one using the actual dose administered to each patient with their specific demographic and empirical Bayes (*post hoc*) estimates from final PopPK models in NONMEM. The concentration sampling times were based on nominal sampling times from DREAMM-2: predose, 0.5, 1, 2, 4, 8, 24, 72, 168, 336, and 504 h after the infusion start. Exposure measures were: maximum concentration for cycle one (C_{max}) for ADC and cys-mcMMAF; average concentration over first 21 days (C_{avg}) for ADC and cys-mcMMAF; minimum concentration at the end of 21-day cycle (C_{tau}) for ADC.

Covariate effects on Cycle 1 ADC and cys-mcMMAF exposure

Simulations were performed using the final model to assess the impact of the significant covariates on cycle 1 C_{max}, C_{avg}, and C_{tau} for ADC and cys-mcMMAF. Simulations were performed using the 2.5-mg/kg dose with typical values of the covariate along the full range of the covariate distribution at specified intervals. Median values were chosen for the continuous covariates to define the typical patient in DREAMM-2: a 65-year-old man weighing 75 kg with mild renal impairment, normal liver function, and sBCMA 100 ng/ml, IgG 10 g/L, and albumin 40 g/L levels at baseline, receiving a 2.5-mg/kg dose. The percent change in the exposure measures at each integer of the covariate from the typical value of the covariate for that patient was calculated. Forest plots were generated to display the impact of covariates on ADC C_{tau} and cys-mcMMAF C_{max}; ADC C_{tau} was shown to be most significant in the exposure–response analyses (Ferron-Brady et al., 2021; in preparation [unpublished data]).

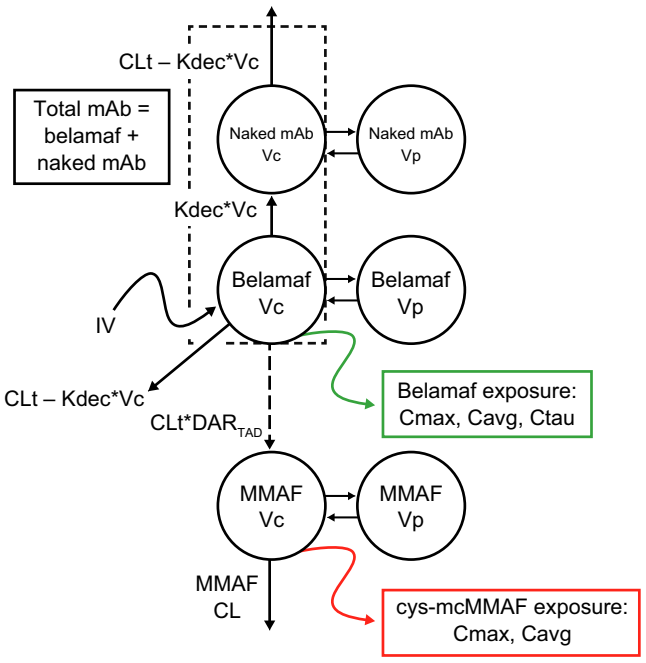

FIGURE 1 Schema for PopPK model development. CL, clearance; CLt, clearance at time (t) since first dose; C_{max}, maximum concentration for cycle one; C_{avg}, average concentration over first 21 days; C_{tau}, minimum concentration at the end of 21-day dosing interval; cys-mcMMAF, cysteine maleimidocaproyl monomethyl auristatin F; DAR, drug-antibody ratio; mAb, monoclonal antibody; PopPK, population pharmacokinetics; TAD, time after dose; Vc, central volume of distribution; Vp, peripheral volume of distribution. Dotted box represents total mAb

RESULTS

Patient population

PopPK analyses included 291 patients (DREAMM-1: $n = 73$; DREAMM-2: $n = 218$) with RRMM (Table S2). Median age was 65 years and 54% of patients were men. Measurable concentrations were obtained from 2248 samples for ADC, 2210 for total mAb, and 286 cys-mcMMAF (VALA method) for DREAMM-1 and 1313 cys-mcMMAF (PKC method) for DREAMM-2.

Population PK model development

A schema of PopPK model development is shown in Figure 1. Analysis of plasma concentration–time data from both studies showed that the time course of ADC and total mAb concentrations were similar with a typical biphasic profile; the difference between total mAb and ADC concentrations increased with the increase in time after last dose. Figure 2 shows data from DREAMM-2. The cys-mcMMAF molar concentrations were significantly lower than ADC and

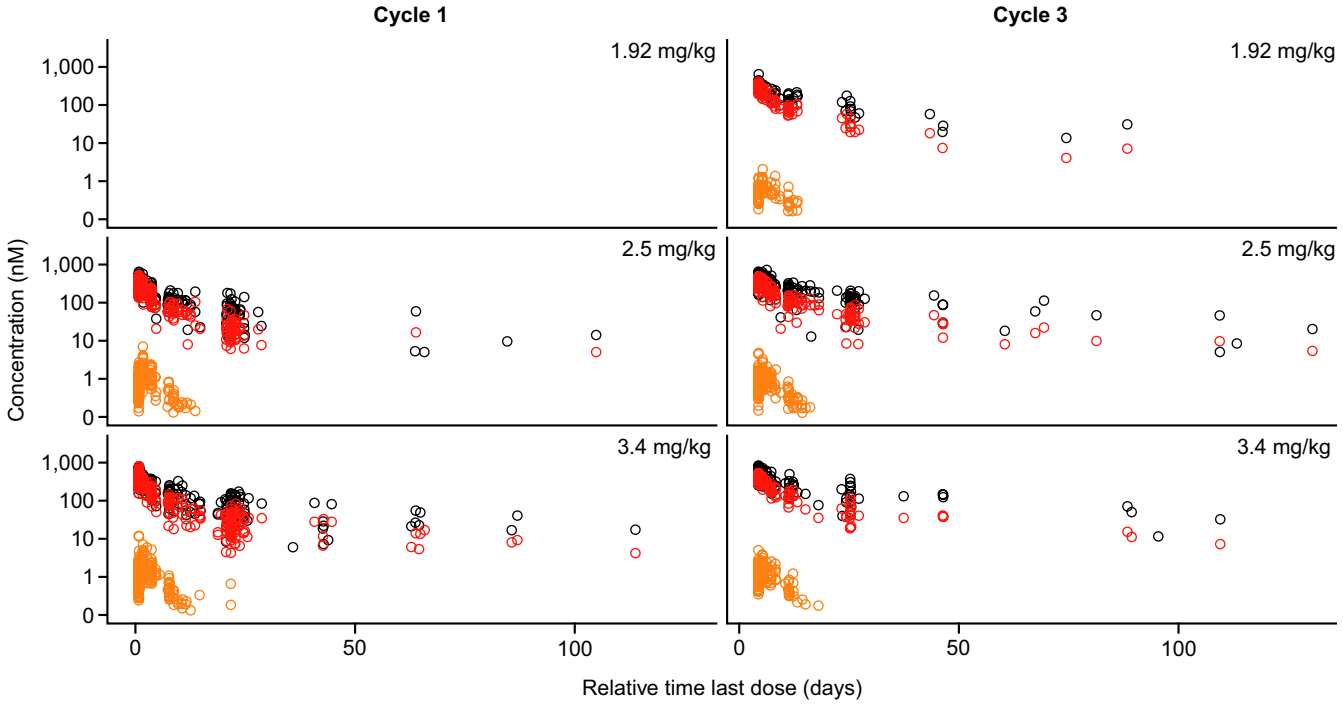

FIGURE 2 Concentration–time profiles for ADC, total mAb, and cys-mcMMAF for cycles one and three in DREAMM-2. Red circles for ADC, black circles for total mAb, and orange circles for cys-mcMMAF. Outliers were excluded from plot. ADC, antibody–drug conjugate; cys-mcMMAF, cysteine maleimidocaproyl monomethyl auristatin F; mAb, monoclonal antibody

total mAb concentrations potentially decreased more rapidly than ADC concentrations, with observed concentrations generally available up to Day 8 post dose.

Population PK model for ADC

The PK parameter estimates from the base and final PopPK models for ADC are shown in Table 1. A linear, two-compartment model with first-order elimination and time-varying CL (described by a sigmoidal time function; Figure 3) best described the PK of ADC. The structural model parameters for the initial model included CL (CLADC), V1, intercompartmental CL, and V2.

Time-varying CL was included in the model using the following equation, consistent with other biologics dosed in patients with cancer[10–12]:

$$CL_{ADC,Time} = CL_{ADC,0} * exp\left(\frac{IMAX * Time^{GAMMA}}{TI50^{GAMMA} + Time^{GAMMA}}\right)$$

where IMAX is maximal change in CL relative to CL at time zero ($CL_{ADC,0}$); TI50 is the time at which 50% of change in CL occurred; and GAMMA is the Hill coefficient.

Using the final individual estimates from the ADC model from DREAMM-2 patients, the CL of ADC decreased over time: the initial ADC typical value (TV) CL was 0.94 L/day with a half-life of 11.5 days; over time, CL was reduced by 28% resulting in a longer half-life of 14.3 days. Time to 50% of maximal change in CL was 51.9 days.

The inclusion of baseline sBCMA, albumin, IgG, and bodyweight, along with dose less than 1 mg/kg and being in the DREAMM-1 study, explained a substantial portion of the between-subject variability (BSV) in CL for the ADC model. Likewise, the inclusion of baseline albumin, bodyweight, gender, dose less than 1 mg/kg, and being in DREAMM-1 described a majority of the BSV for central volume of ADC; inclusion of covariates in the final model resulted in decreased interindividual variability (expressed as coefficient of variation) from 58.4% to 34.1% for CL, from 27.9% to 14.6% for V1, and from 82.2% to 55.6% for V2.

The final ADC model described the data well as indicated by goodness of fit (GOF; Figure S1a), normal prediction distribution error (NPDE), ETA versus covariate, and individual fit plots; bootstrap results demonstrated adequate model stability (Table 1). The VPC for ADC illustrates the robustness of the model to describe both 2.5- and 3.4-mg/kg doses (Figure 4a).

Population PK model for total mAb

Base and final total mAb PopPK model results are shown in Table S3. Similar to the ADC model, the total mAb model characterized the distribution and elimination of the analytes with linear two-compartment kinetics. As the only difference

TABLE 1 PK parameter estimates for the final PopPK model for ADC

PK parameter (unit)	Final model	
	Theta	95% CI
TVCL (L/day)	0.94	0.87, 1.00
TVV1 (L)	4.47	4.34, 4.61
TVQ (L/day)	0.78	0.70, 0.88
TVV2 (L)	5.96	5.52, 6.47
IMAX	–0.33	–0.44, –0.24
TI50 (day)	53.90	46.90, 64.40
GAMMA	4.30	3.01, 8.02
Effect of BWT on V1 (θ_{V1_BWT})	0.50	0.41, 0.58
Effect of BWT on CL (θ_{CL_BWT})	0.51	0.27, 0.71
Effect of BALB on CL (θ_{CL_BALB})	–0.97	–1.64, –0.25
Effect of BALB on V1 (θ_{V1_BALB})	–0.47	–0.60, –0.33
Effect of male sex on V1 (θ_{V1_SEX})	1.14	1.09, 1.18
Effect of BSBCMA on CL (θ_{CL_BSBCMA})	0.13	0.09, 0.17
Effect of BIGG on CL (θ_{CL_BIGG})	0.13	0.09, 0.16
Effect of dose <1 mg/kg on V2 ($\theta_{V2\_ADOSE<1}$)	0.13	0.02, 0.29
Effect of dose <1 mg/kg on CL ($\theta_{CL\_ADOSE<1}$)	0.62	0.46, 0.86
Effect of DREAMM1/BMA117159 on V1 ($\theta_{V1\_DREAMM1}$)	0.66	0.63, 0.70
Effect of DREAMM1/BMA117159 on CL ($\theta_{CL\_DREAMM1}$)	0.61	0.53, 0.70
ETACL (%)	35.00	26.70, 40.10
ETAV1 (%)	14.60	12.60, 16.30
ETAQ (%)	37.80	17.90, 49.50
ETAV2 (%)	46.80	32.60, 60.50
ETAIMAX (%)	123.00	76.10, 199.0
ETATI50 (%)	30.10	18.80, 39.50
RES ERR, additive SIGMA on log scale	0.019	0.016, 0.023

Lower 95% CI and upper 95% CI were calculated using bootstrap; 1219 of the 2000 bootstrap runs minimized successfully.

ε, residual error; ADC, antibody–drug conjugate; BALB, baseline albumin; BIGG, baseline immunoglobulin G; BSBCMA, baseline soluble BCMA; BWT, body weight; CI, confidence interval; CL, clearance; ETA (η), inter-individual variability; I, individual patient parameter; IMAX, maximal change in CL relative to baseline; PK, pharmacokinetic; PopPK, population pharmacokinetics; Q, inter-compartmental clearance; %RSE, percent relative standard error; SE, standard error; TI50, time at which 50% of change in CL has occurred; TV, typical value; V1, central volume of distribution, V2, peripheral volume of distribution.

between the naked mAb and the ADC is the lack of a small number of cys-mcMMAF molecules, it was hypothesized that this would not impact the mAb PK characteristics; the central and peripheral volume of distribution, as well as the elimination and distribution CL, for the naked mAb were kept the same as for ADC. When generating the base model, a consistent underestimation of total mAb concentration was observed, even at early time points, possibly due to differences in assays used to measure ADC and total mAb. To account for this apparent underestimation, a correction factor, CORR, was introduced into the total mAb model where IPRED are individual predictions:

$$IPRED_{Total\ mAb} = CORR * (IPRED_{ADC} + IPRED_{Naked\ mAB})$$

A similar use of a correction factor was previously used to correct for systemic bias in the model fitting of total mAb and ADC concentrations for another ADC.[13] VPC (Figure 4b), GOF (Figure S1b), NPDE, ETA versus covariate, and individual fit plots showed that the model adequately described the total mAb concentration data.

Population model for cys-mcMMAF

The final cys-mcMMAF PopPK model results are shown in Table S4. A linear two-compartment model with first-order elimination kinetics was used to describe cys-mcMMAF plasma concentrations linked to ADC. The input rate was governed by the proteolytic degradation and deconjugation rates of ADC and was modulated by an empirical drug antibody ratio (DAR) term that declined exponentially over time following each dose (TAD); the DAR was reset to the drug product DAR value, DAR_0, with each dose (Figure 1). The DAR was calculated as follows, using the time since the most recent dose and the rate of decrease of DAR with time (RATE):

$$DAR_{TAD} = DAR_0 * EXP(-RATE * TAD)$$

For cys-mcMMAF, ~ 25% of samples collected after the first dose were below the lower limit of quantification (BLOQ) for either assay. Most BLOQ samples occurred prior to each dose (ie, ~21 days after the previous dose). Over 90% of these predose samples were BLOQ; they were not anticipated to be informative. With a relatively short estimated half-life (10 min to 14 h, for the alpha and beta phase, respectively) and low C_{max} levels of cys-mcMMAF, most of the PK information was within 7 days after dosing. The likelihood-based M3 method[14] was evaluated on the final model, and little difference was observed in individual predicted profiles; no major impact on exposure measures was observed. The time to 50% reduction in DAR was 10.3 days after dosing. Additionally, interoccasion variability was included on both CL and central volume of cys-mcMMAF to describe the difference in profiles for different cycles.

The final model for cys-mcMMAF included baseline sBCMA and IgG covariates, which impacted the central

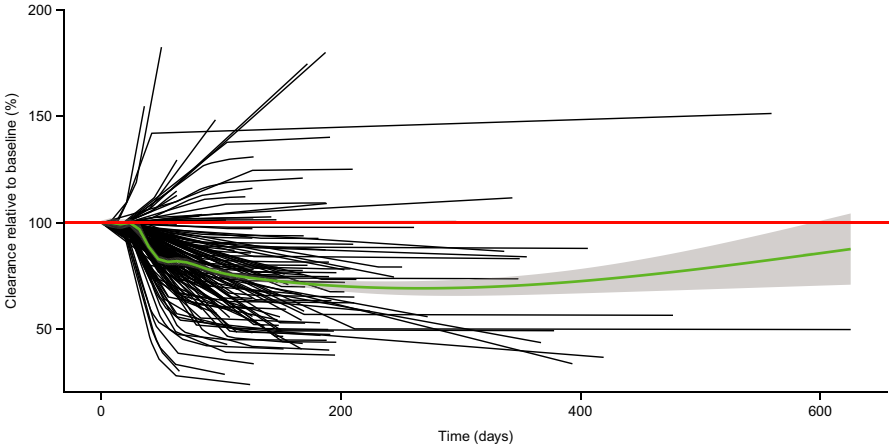

FIGURE 3 Time change in ADC CL relative to baseline as predicted by the final model with time varying CL. Red line represents no change from baseline clearance; green line with shaded ribbon represents the locally estimated scatterplot smoothing (LOESS) line and its 95% confidence interval. ADC, antibody–drug conjugate; CL, clearance

volume of cys-mcMMAF. These covariates were significant but had less impact on the BSV compared with ADC. The final cys-mcMMAF model described the data well, as indicated by GOF (Figure S1c) and VPC plots (Figure 4c). Covariates of clinical interest, such as mild to moderate renal impairment, mild hepatic impairment, age, ethnicity, African American race, and prior treatments, did not have a significant impact on the PK parameters for ADC or cys-mcMMAF.

Modeling post hoc exposure measures

Cycle one exposures in the study were computed using the final PopPK models for ADC and cys-mcMMAF. There was a strong positive correlation between ADC C_{avg} and ADC C_{tau} and weaker positive correlations between ADC C_{max} and ADC C_{tau}, as well as weaker correlations between cys-mcMMAF C_{max} and ADC C_{max} across the whole analysis population. Exploring the relationship of ADC C_{tau}, there was an inverse relationship with baseline sBCMA, IgG, or β_2-microglobulin, but a positive relationship with baseline albumin (Figure S2); bodyweight had a lesser impact on ADC C_{tau}. There was substantial overlap between exposure at 2.5- and 3.4-mg/kg doses for the frozen liquid presentation, consistent with the small difference in dose level and the observed BSV in DREAMM-2 (Figure S3). The median ADC C_{tau} was higher for the 24 patients receiving the lyophilized 3.4 mg/kg presentation (Figure S3), which can be explained by the lower levels of baseline sBCMA and IgG in that cohort.

Typical patient and impact of covariates on exposure measures

Implementing values from a typical DREAMM-2 patient into the final ADC and cys-mcMMAF models obtained the following calculated exposures after a dose of 2.5 mg/kg: ADC C_{max}, C_{avg}, and C_{tau} of 36.5 μg/ml, 7.76 μg/ml, and 2.22 μg/ml, respectively; cys-mcMMAF C_{max} and C_{avg} of 917 pg/ml and 217 pg/ml, respectively. The values would be 1.36 times higher in patients receiving a 3.4-mg/kg dose.

The impact of differences in baseline covariates on exposure was assessed by plotting the percent change from the typical patient value (Figure 5). Baseline sBCMA, IgG, and albumin were significant for ADC from a PK perspective as ADC C_{tau} deviated for the 5th and 95th percentiles of the covariate distribution by more than 30% from typical patient values. In general, the covariate impact was smaller (<30% difference corresponding to 5th and 95th percentiles) for cys-mcMMAF exposure measures, with the exception of bodyweight. A patient with a very low baseline sBCMA level would have a 50% higher ADC Ctau compared with a typical patient, whereas a patient with a high baseline sBCMA level (eg, 500 ng/ml) would have a 35% lower C_{tau} (Figure 5a). Baseline IgG also had a large effect on ADC C_{tau} (Figure 5b), with smaller effects for baseline albumin (Figure 5c) and bodyweight (Figure 5d).

The forest plots of ADC Ctau and cys-mcMMAF Cmax (normalized to 2.5-mg/kg dose) showed no significant differences across the potentially important clinical covariates of age, gender, race, renal function classification, and hepatic function (Figure 6). The largest deviation from geometric mean value of the entire population was at very low albumin and very high baseline IgG levels. There was a trend for higher cys-mcMMAF C_{max} in African American patients, possibly related to a greater proportion of these patients having low activity of OATP1B3, a transporter of cys-mcMMAF; however, patient numbers were small. Figure 6 shows that patients with low activity of OATP1B3 have increased cys-mcMMAF C_{max}. As transporter activity was unknown for ~ 45% of the patients, with a limited number of patients with

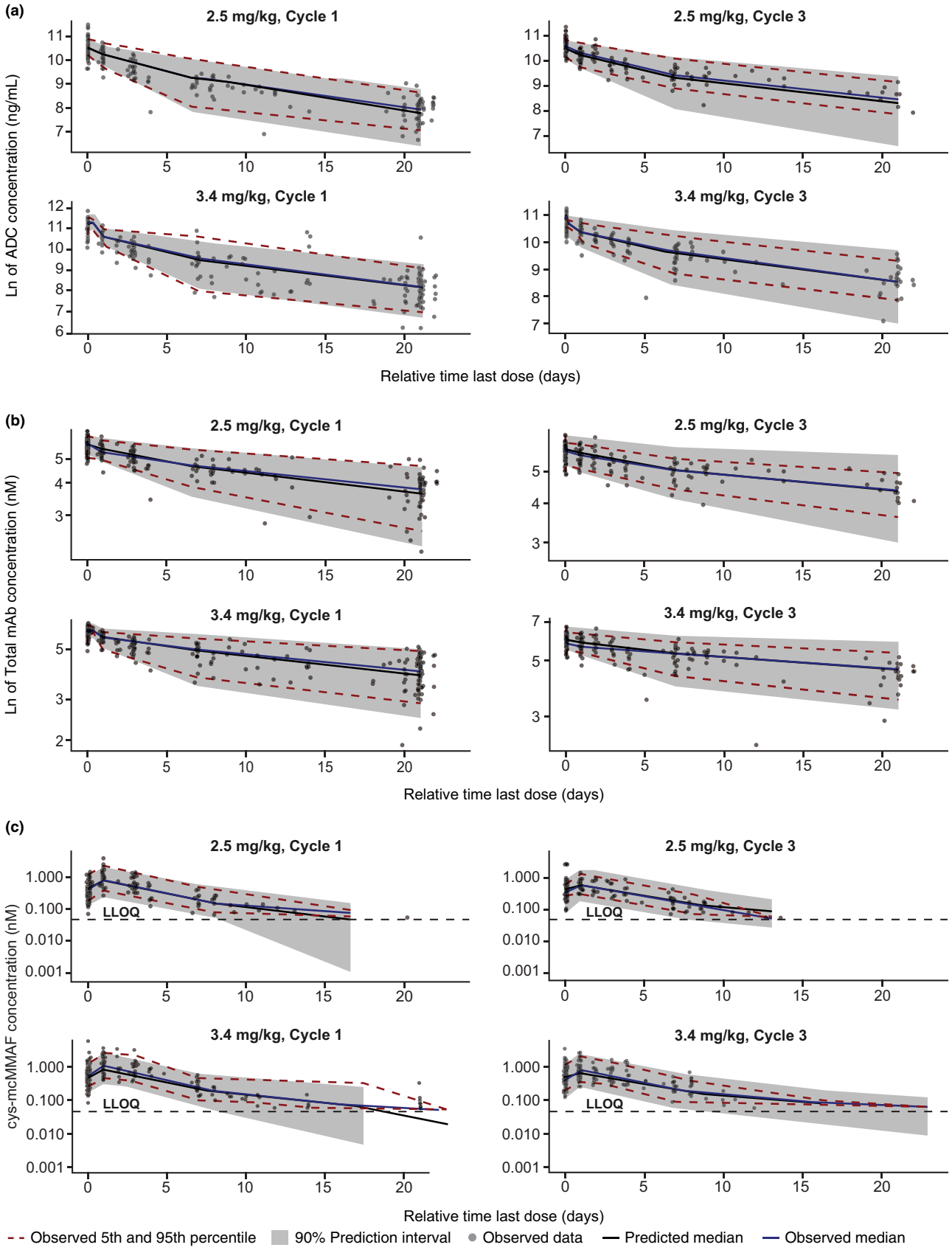

FIGURE 4 Final model VPC plots for (a) ADC, (b) total mAb, and (c) cys-mcMMAF by belamaf dose and cycle. ADC, antibody–drug conjugate; cys-mcMMAF, cysteine maleimidocaproyl-MMAF; LLOQ, lower limit of quantification; mAb, monoclonal antibody; VPC, visual predictive check

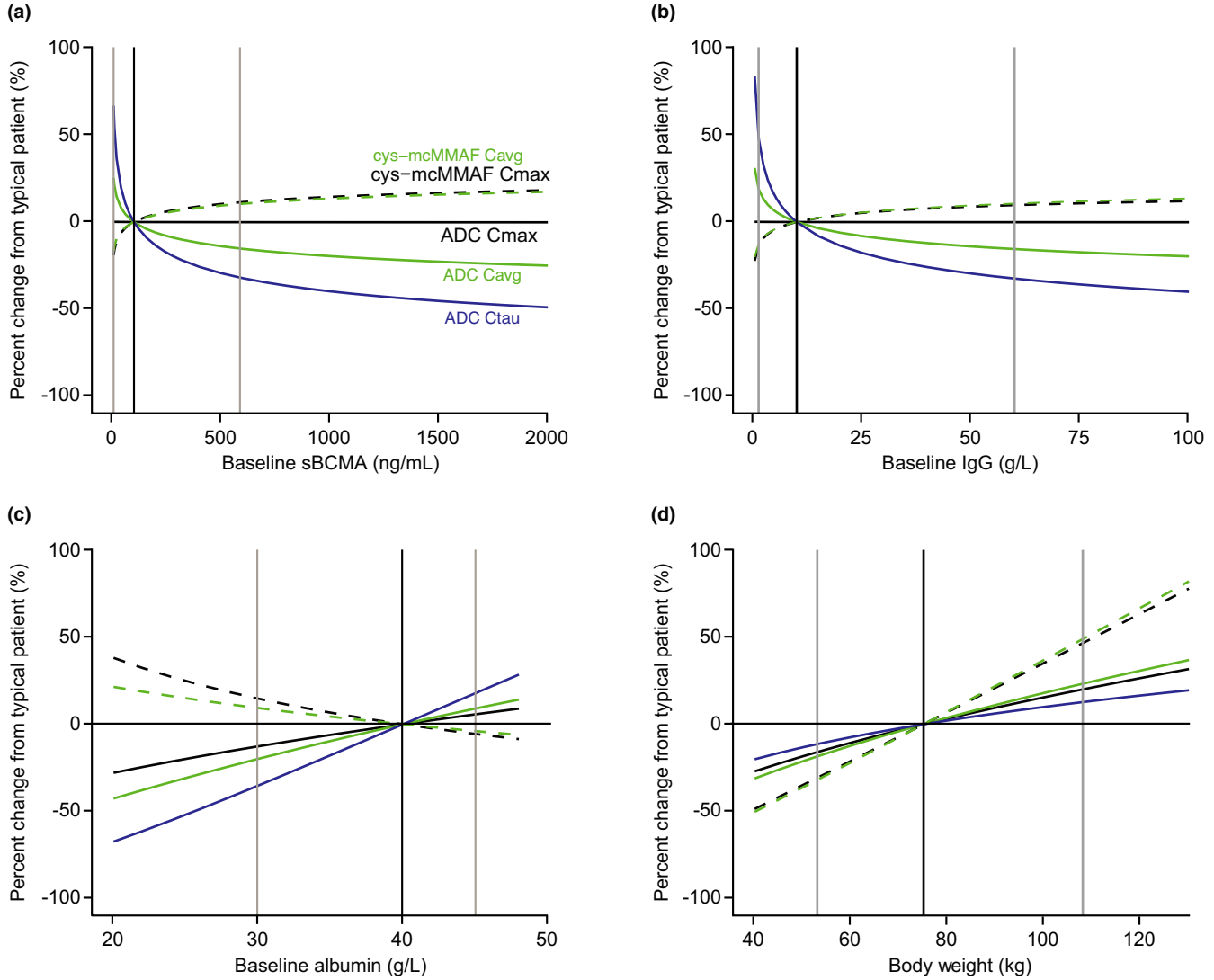

FIGURE 5 Impact of significant covariates at baseline on ADC and cys-mcMMAF exposure measures using final ADC and cys-mcMMAF PopPK models: (a) sBCMA, (b) IgG, (c) albumin, and (d) bodyweight. Dark vertical lines represent the typical patient from DREAMM-2. The light vertical lines represent the 5th and 95th percentiles. ADC, antibody–drug conjugate; C_{max}, maximum concentration for cycle one; C_{avg}, average concentration over first 21 days; C_{tau}, minimum concentration at the end of 21-day dosing interval; cys-mcMMAF, cysteine maleimidocaproyl monomethyl auristatin F; IgG, immunoglobulin; PopPK, population pharmacokinetics; sBCMA, soluble B-cell maturation antigen

low OATP1B3 activity, further evaluation of the impact of transporter activity on cys-mcMMAF elimination in future studies is warranted.

DISCUSSION

The PopPK analysis of belamaf ADC, total mAb, and cys-mcMMAF concentrations from DREAMM-1 and DREAMM-2 provides a valuable assessment of covariates that impact exposure. The PopPK models characterized the PK of ADC, total mAb, and cys-mcMMAF well-described by linear, two-compartment models, consistent with ADC and mAb PK models reported elsewhere,[15] with time-varying CL for ADC and time-varying DAR for cys-mcMMAF.[10,16,17]

PK parameter estimates were in the range of those described for other mAbs in patients with malignancies, including the findings of decreasing CL over time, as well as the maximum decrease and time to 50% decrease.[10–12,16,18] Mean maximum decreases in CL of 24.5% have been reported for nivolumab in solid tumor studies,[19] 20% for pembrolizumab in melanoma and non-small cell lung carcinoma (NSCLC),[12] 17.1% for atezolizumab in NSCLC,[19] and 50% for isatuximab linear clearance in MM.[20] Time-varying CL may be related to a reduction in inflammation or metabolic stress, which subsequently manifests itself in decreased catabolism of mAb as a result of the drug's therapeutic effects.[21] Another potential explanation could be the reduction in antigen burden, which would also result in a decrease in CL with time.[16] Supporting these hypotheses, the magnitude of reduction in CL has been reported to be higher in responders than in nonresponders for nivolumab, pembrolizumab,

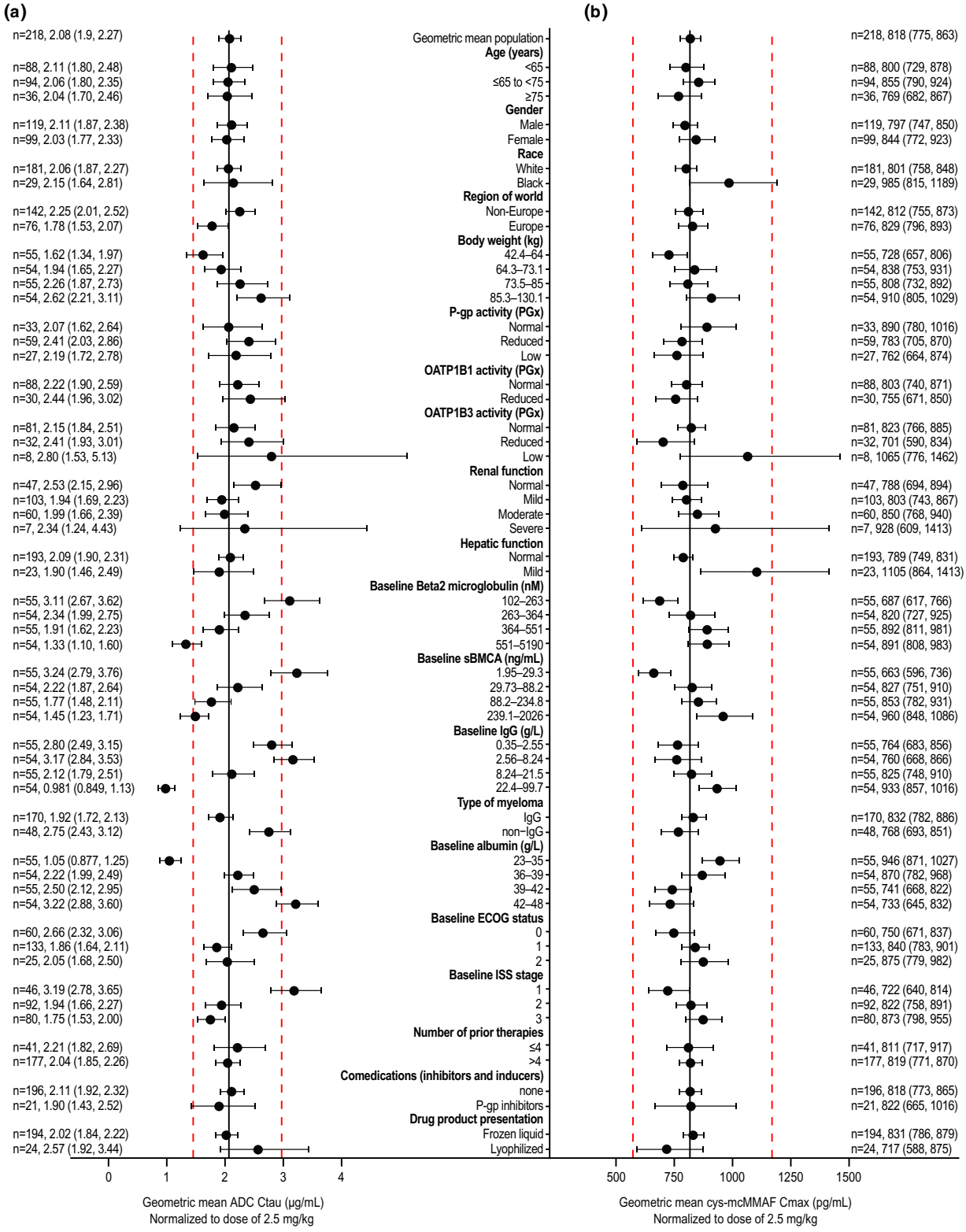

FIGURE 6 Forest plots of *post hoc* exposure of (a) ADC (cycle 1) C_{tau} exposure and (b) cys-mcMMAF C_{max} in various subgroup populations (DREAMM-2). Solid black circles represent geometric mean and error bar represents 95% confidence interval. Solid black lines represent the geometric mean value of all patients. Dashed red lines represent an interval of 0.7 to 1.43 times the geometric mean of all patients. The n = sample size and numbers represent geometric mean and 95% confidence interval for that subgroup. All the patient exposures were normalized to 2.5-mg/kg dose. Subgroups with less than five patients were omitted from plot. Missing data were imputed at the median value for the population, except for PGx activity where unknowns were left uncategorized. ADC, antibody–drug conjugate; C_{max}, maximum concentration after dose; C_{tau}, minimum concentration at the end 21-day dosing interval; cys-mcMMAF, cysteine maleimidocaproyl monomethyl auristatin F; ECOG, Eastern Cooperative Oncology Group; IgG, immunoglobulin; ISS, International Staging System; P-gp, P-glycoprotein; sBCMA, soluble B-cell maturation antigen

and avelumab.[11,12,16] In our DREAMM-2 study (Figure S4), there was a small trend for a higher reduction in clearance in responders.

Baseline sBCMA and IgG were the most significant factors associated with ADC exposure, followed to a lower extent by baseline albumin level and bodyweight. All three of the strongest ADC covariate effects are related to disease state; patients with worse disease state and prognosis (higher sBCMA and IgG, lower albumin) have higher CL and consequently lower ADC C_{tau} and C_{avg} exposure. The impact of a covariate on ADC exposure tended to have the opposite effect on cys-mcMMAF exposure, except for bodyweight; this may be related to the fact that cys-mcMMAF is generated in part by ADC CL (ie, internalization and release from killed target cells). IgG covariate effects on CL were previously identified for other mAbs in cancers with increased IgG levels, such as RRMM of IgG-type.[22] The increase of CL with higher IgG levels is likely related to neonatal Fc receptor (FcRn) mediated recycling of endogenous IgG and IgG-type mAbs,[23] whereby increased endogenous IgG levels lead to increased competition for the FcRn receptor in the endosome, leading to decreased recycling of ADC and subsequently increased lysosomal degradation and systemic CL.

Belamaf ADC half-life was estimated to be between 11.5 and 14.0 days, which is similar to or longer than the half-life of other ADCs.[24–26] The formation of antidrug antibodies against the ADC is not thought to contribute to the lower half-life, as the immunogenicity of belamaf was shown to be very low (<1%).[1]

There was a notable difference in exposure between the two DREAMM studies after accounting for the effect of other covariates, with higher ADC exposure observed in DREAMM-1. Overall, no major differences in exposure were observed across the clinical covariates of age, gender, race, renal function classification, and hepatic function, suggesting that any differences in these baseline characteristics between studies would not contribute significantly to PK variation. It is possible that the observed effect is partly related to differences between the studies in the proportion of patients who received prior anti-CD38 treatment; in a PopPK model of avelumab, previous use of biologics was associated with a small reduction in CL and central volume of distribution.[16] Differences in CL may be due to between-study analytical/process differences (ie, assays used). The reasons for exposure differences between DREAMM-1 and DREAMM-2 remain unclear.

There was a pronounced effect of dose on ADC PK, with doses less than 1 mg/kg associated with lower CL and volume of distribution; similar observations have been reported for other mAbs.[27] Only a limited number of patients received such low doses, all of whom were from DREAMM-1. The slower CL at lower doses is unlikely to result from target-mediated drug disposition as a disproportionately low ADC area under the curve (AUC) was not observed in patients receiving lower doses in DREAMM-1. The effect of dose was included to reduce the unexplained BSV and improve the VPC; therefore, general mechanistic inferences should not be drawn based on the compensatory effects in the context of the pooled PK dataset with most patients and samples coming from DREAMM-2.

The deconjugation rate constant (Kdec) in the total mAb model was estimated to be 0.059, which is similar to what was reported for depatux-m (0.0539/day), an ADC with the same linker and payload.[15]

Limitations of this PopPK modeling analysis include the small number of patients receiving lower doses of belamaf (and this was only in one study), unanswered questions around the between-study and low-dose effects, and the relatively low number of measurable concentrations available at later timepoints for cys-mcMMAF. However, the models had considerable validity and stability, as determined by GOF, NPDE, VPC plots, and bootstrapping methods. The models were also able to identify covariates that impacted meaningfully on PK parameters. Relevant exposure measures have been utilized in exposure–response modeling to assess relationship between ADC and cys-mcMMAF exposure and key efficacy and safety end points, as reported elsewhere (Ferron-Brady et al., 2021; in preparation [unpublished data]).

ADC C_{tau} was inversely related to baseline sBCMA and IgG and overlapped between the two doses (2.5 and 3.4 mg/kg) evaluated in DREAMM-2. This overlap was partially explained by variations in baseline levels of sBCMA and IgG between the two dose groups; there was no observed nonlinearity in dosing above 1 mg/kg. ADC and cys-mcMMAF PK were not impacted by mild to moderate renal impairment, mild hepatic impairment, age, ethnicity, African American race, nor prior treatments. The ADC presentation (frozen liquid or lyophilized) did not have a significant impact on the PK parameters in the covariate analysis.

In summary, belamaf ADC, total mAb, and cys-mcMMAF concentration-time profiles were well-described by their respective PK models. Belamaf ADC exhibited time-varying clearance consistent with other monoclonal antibodies used in oncology. Disease burden and patient characteristics, including baseline IgG, sBCMA, albumin, and body weight, were identified as significant covariates. Mild to moderate renal impairment, mild hepatic impairment, age, African American race, prior treatments, and lyophile presentation were not found to significantly impact belamaf ADC, total mAb, or cys-mcMMAF PK.

ACKNOWLEDGEMENTS

Drug linker technology was licensed from Seagen, Inc. (Bothell, WA, USA) and the monoclonal antibody was produced with POTELLIGENT Technology licensed from

BioWa (Princeton, NJ, USA). Trademarks are owned by or licensed to the GSK group of companies. The authors would like to thank Jan van der Linde and Priyanka Kocheta from Parexel International for dataset preparation. Editorial support (in the form of writing assistance, including preparation of the draft manuscript under the direction and guidance of the authors, collating, and incorporating authors' comments for each draft, assembling tables and figures, grammatical editing, and referencing) was provided by Mark Powell, Fishawack Indicia Ltd., UK, part of Fishawack Health, and funded by GSK.

CONFLICTS OF INTEREST

C.R., J.C., H.S., J.O., and G.F.-B. are employees of GSK and hold ownership interests. R.C.J. is an employee of GSK and holds ownership interests in GSK and Novartis.

AUTHOR CONTRIBUTIONS

All authors wrote the manuscript, designed the research, performed the research, and analyzed the data.

DATA AVAILABILITY STATEMENT

Anonymized individual participant data and study documents can be requested for further research from www.clinicalstudydatarequest.com.

REFERENCES

1. Food and Drug Administration (FDA). BLENREP prescribing information (US). 2020. https://www.accessdata.fda.gov/drugsatfda_docs/label/2020/761158s000lbl.pdf. Accessed April 21, 2021.
2. European Medicines Agency (EMA). BLENREP Summary of Product Characteristics (EU). 2020. https://www.ema.europa.eu/en/documents/product-information/blenrep-epar-product-information_en.pdf. Accessed April 21, 2021.
3. Tai YT, Mayes PA, Acharya C, et al. Novel anti-B-cell maturation antigen antibody-drug conjugate (GSK2857916) selectively induces killing of multiple myeloma. *Blood*. 2014;123:3128-3138.
4. Tai YT, Anderson KC. Targeting B-cell maturation antigen in multiple myeloma. *Immunotherapy*. 2015;7:1187-1199.
5. Montes de Oca R, Bhattacharya S, Vitali N, et al. The anti-BCMA antibody-drug conjugate belantamab mafodotin drives immunogenic cell death and immune-mediated anti-tumor responses and in combination with an OX40 agonist potentiates in vivo activity. *Euro Hematol Association Library*. 2019; 266357; PF558.
6. Trudel S, Lendvai N, Popat R, et al. Antibody-drug conjugate, GSK2857916, in relapsed/refractory multiple myeloma: an update on safety and efficacy from dose expansion phase I study. *Blood Cancer J*. 2019;9:37.
7. Trudel S, Lendvai N, Popat R, et al. Targeting B-cell maturation antigen with GSK2857916 antibody-drug conjugate in relapsed or refractory multiple myeloma (BMA117159): a dose escalation and expansion phase 1 trial. *Lancet Oncol*. 2018;19:1641-1653.
8. Lonial S, Lee HC, Badros A, et al. Belantamab mafodotin for relapsed or refractory multiple myeloma (DREAMM-2): a two-arm, randomised, open-label, phase 2 study. *Lancet Oncol*. 2020;21:207-221.
9. Patel H, Egorin MJ, Remick SC, et al. Comparison of Child-Pugh (CP) criteria and NCI organ dysfunction working group (NCI-ODWG) criteria for hepatic dysfunction (HD): Implications for chemotherapy dosing. *J Clin Oncol*. 2004;22:6051.
10. Sanghavi K, Zhang J, Zhao X, et al. Population pharmacokinetics of ipilimumab in combination with nivolumab in patients with advanced solid tumors. *CPT Pharmacometrics Syst Pharmacol*. 2020;9:29-39.
11. Liu C, Li H, Liu J, et al. Association of time-varying clearance of nivolumab with disease dynamics and its implications on exposure response analysis. *Clin Pharmacol Ther*. 2017;101:657-666.
12. Li H, Yu J, Liu C, et al. Time dependent pharmacokinetics of pembrolizumab in patients with solid tumor and its correlation with best overall response. *J Pharmacokinet Pharmacodyn*. 2017;44:403-414.
13. Lu D, Gibiansky L, Agarwal P, et al. Integrated two-analyte population pharmacokinetic model for antibody-drug conjugates in patients: implications for reducing pharmacokinetic sampling. *CPT Pharmacometrics Syst Pharmacol*. 2016;5:665-673.
14. Ahn JE, Karlsson MO, Dunne A, Ludden TM. Likelihood based approaches to handling data below the quantification limit using NONMEM VI. *J Pharmacokinet Pharmacodyn*. 2008;35:401-421.
15. Mittapalli RK, Stodtmann S, Friedel A, et al. An integrated population pharmacokinetic model versus individual models of depatuxizumab mafodotin, an anti-EGFR antibody drug conjugate, in patients with solid tumors likely to overexpress EGFR. *J Clin Pharmacol*. 2019;59:1225-1235.
16. Wilkins JJ, Brockhaus B, Dai H, et al. Time-varying clearance and impact of disease state on the pharmacokinetics of avelumab in Merkel cell carcinoma and urothelial carcinoma. *CPT Pharmacometrics Syst Pharmacol*. 2019;8:415-427.
17. Ahamadi M, Freshwater T, Prohn M, et al. Model-based characterization of the pharmacokinetics of pembrolizumab: a humanized anti-PD-1 monoclonal antibody in advanced solid tumors. *CPT Pharmacometrics Syst Pharmacol*. 2017;6:49-57.
18. Bajaj G, Wang X, Agrawal S, Gupta M, Roy A, Feng Y. Model-based population pharmacokinetic analysis of nivolumab in patients with solid tumors. *CPT Pharmacometrics Syst Pharmacol*. 2017;6:58-66.
19. Hamuro L, Statkevich P, Bello A, Roy A, Bajaj G. Nivolumab clearance is stationary in patients with resected melanoma on adjuvant therapy: implications of disease status on time-varying clearance. *Clin Pharmacol Ther*. 2019;106:1018-1027.
20. Fau JB, El-Cheikh R, Brillac C, et al. Drug-disease interaction and time-dependent population pharmacokinetics of isatuximab in relapsed/refractory multiple myeloma patients. *CPT Pharmacometrics Syst Pharmacol*. 2020;9:649-658.
21. Turner DC, Kondic AG, Anderson KM et al. Pembrolizumab exposure-response assessments challenged by association of cancer cachexia and catabolic clearance. *Clin Cancer Res*. 2018;24:5841-5849.
22. Yan X, Clemens PL, Puchalski T et al. Influence of disease and patient characteristics on daratumumab exposure and clinical outcomes in relapsed or refractory multiple myeloma. *Clin Pharmacokinet*. 2018;57:529-538.
23. Souders CA, Nelson SC, Wang Y, Crowley AR, Klempner MS, Thomas W Jr. A novel in vitro assay to predict neonatal Fc receptor-mediated human IgG half-life. *MAbs*. 2015;7:912-921.

24. Younes A, Kim S, Romaguera J et al. Phase I multidose-escalation study of the anti-CD19 maytansinoid immunoconjugate SAR3419 administered by intravenous infusion every 3 weeks to patients with relapsed/refractory B-cell lymphoma. *J Clin Oncol*. 2012;30:2776-2782.
25. Astellas Pharma. Enfortumab vedotin (PADCEV) prescribing information. 2021. https://astellas.us/docs/PADCEV_label.pdf. Accessed April 21, 2021.
26. Genentech. Polatuzumab vedotin (POLIVY) prescribing information. 2020. https://www.gene.com/download/pdf/polivy_prescribing.pdf. Accessed April 21, 2021
27. Bensalem A, Ternant D. Pharmacokinetic variability of therapeutic antibodies in humans: a comprehensive review of population pharmacokinetic modeling publications. *Clin Pharmacokinet*. 2020;59:857-874.

SUPPORTING INFORMATION

Additional supporting information may be found online in the Supporting Information section.

How to cite this article: Rathi C, Collins J, Struemper H, Opalinska J, Jewell RC, Ferron-Brady G. Population pharmacokinetics of belantamab mafodotin, a BCMA-targeting agent in patients with relapsed/refractory multiple myeloma. *CPT Pharmacometrics Syst Pharmacol*. 2021;10:851–863. https://doi.org/10.1002/psp4.12660